Supporting Information

Graphene highly-scattered in porous carbon nanofibers: a binder-free and high-performance anode for sodium-ion batteries

Yongchang Liu,[ab] Li-Zhen Fan*[a] and Lifang Jiao*[b]

[a]Institute of Advanced Materials and Technology, University of Science and Technology Beijing, Beijing 100083, China. E-mail: fanlizhen@ustb.edu.cn

[b]Key Laboratory of Advanced Energy Materials Chemistry (Ministry of Education), Nankai University, Tianjin 300071, China. E-mail: jiaolf@nankai.edu.cn

Supplementary Figures

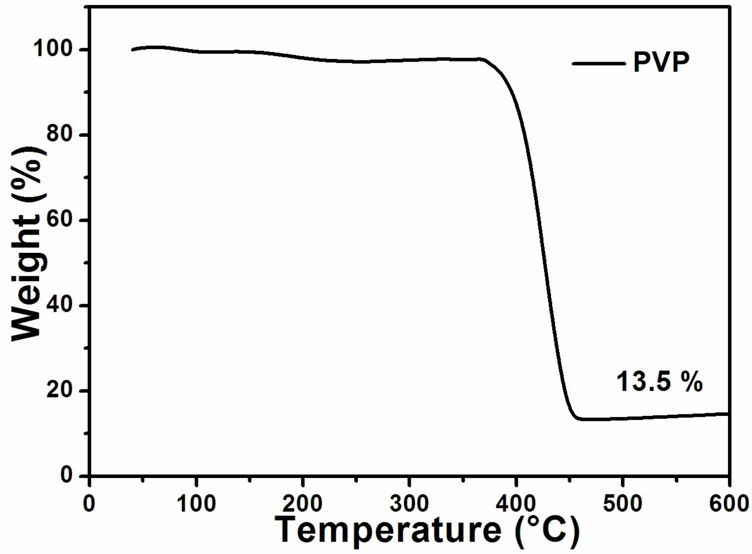

Fig. S1 TGA curve of PVP in high purity Ar atmosphere from room temperature to 600 °C with a heating rate of 5 °C min^{-1}.

The only 2.3% weight loss observed until 365 °C is attributed to the evaporation of adsorbed water. This indicates that PVP is stable in inert atmosphere up to 365 °C. The fast weight loss from 365 to 460 °C is assigned to the decomposition and carbonization of PVP. The residual carbon mass is about 13.5% of the pristine PVP mass.

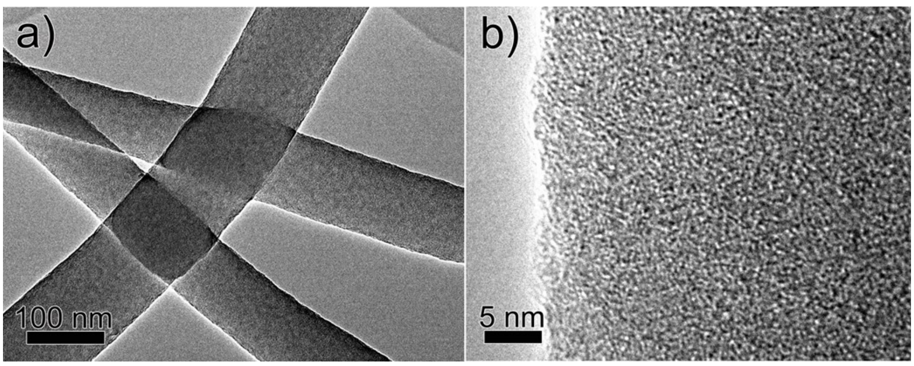

Fig. S2 (a) TEM and (b) HRTEM images of the blank porous carbon nannofibers fabricated by heat treating the electrospun PVP at 500 °C for 1 h.

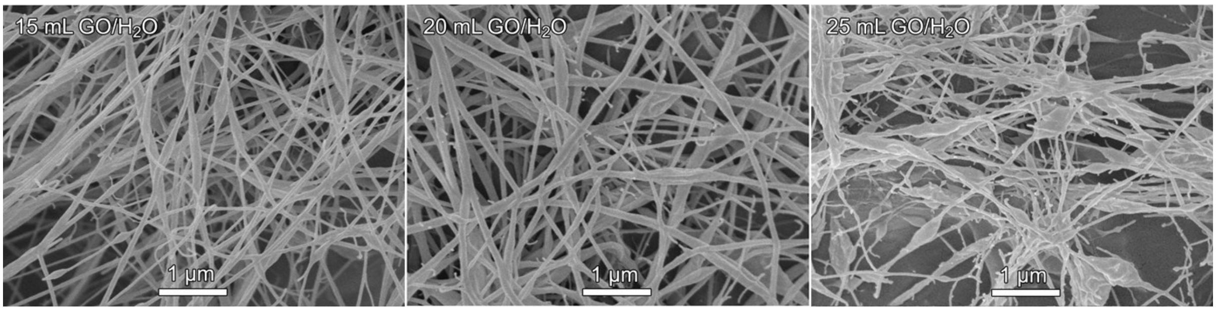

Fig. S3 SEM images of the as-spun GO/PVP nanofibers prepared from different spinning solutions: 15 mL, 20 mL, and 25 mL GO/H_2O dispersion with 1.2 g PVP.

The nanofibers electrospun from 15 mL GO/H_2O with 1.2 g PVP are thinner than those from 20 mL GO/H_2O with 1.2 g PVP, due to the insufficient GO content. While, excessive GO cannot be totally wrapped by PVP nanofibers (25 mL GO/H_2O with 1.2 g PVP). Appropriate dosage ratio (20 mL GO/H_2O with 1.2 g PVP) is very important for obtaining the smooth and continuous precursor nanofibers.

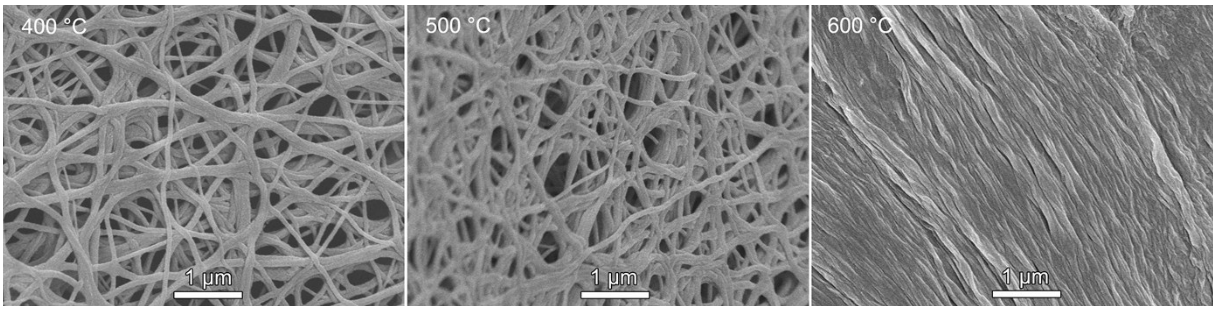

Fig. S4 SEM images of the carbonized GO/PVP nanofibers after calcination at 400, 500, and 600 °C for 1 h.

The nanofibers calcinated at 400 °C are thicker than those calcinated at 500 °C, suggesting that a low temperature cannot completely decompose the PVP to carbon (consistent with the thermogravimetric analysis in Fig. S1). While, a high temperature (600 °C) results in aggregated large areas of graphene that is coated on the surface of carbon nanofibers. Consequently, 500 °C is the best carbonization temperature.

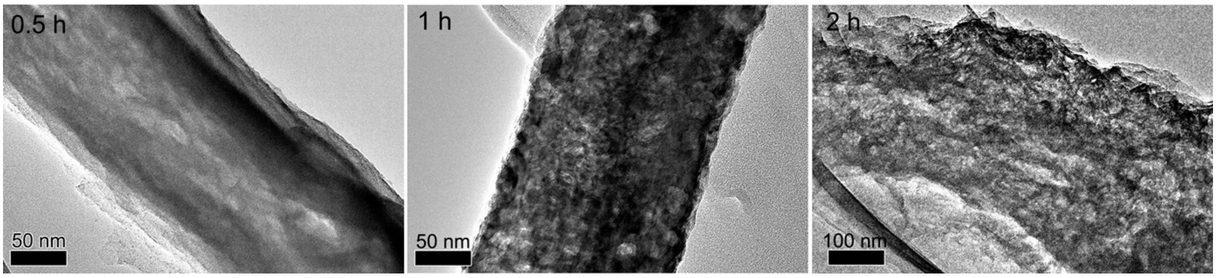

Fig. S5 TEM images of the carbonized GO/PVP nanofibers after calcination at 500 °C for 0.5, 1, and 2 h.

The graphene nanoflakes calcinated for 0.5 h are not in full bloom compared with those calcinated for 1 h. While, a long calcinating time (2 h) leads to the agglomeration of graphene that is extended beyond the carbon nanofibers. Therefore, 1 h is the best carbonization time.

Determination of the graphene percentage in the G/C composite

In the electrospinning fluid, 20 mL GO/H_2O dispersion (concentration: 5 mg mL^{-1}) contains 100 mg GO, in which the oxygen content is 30.76 mg and the carbon content is 69.24 mg. After the heat treatment, assuming the G/C mass is *x* mg, thereby the oxygen content is *x*×2.93% mg, and the carbon content is *x*×(1-2.93%) mg. Considering 1.2 g PVP results in 162 mg (1200 mg×13.5 %) carbon nanofibers, it can be concluded that *x*×(1-2.93%) = 69.24 + 162 mg, so *x* = 238.22 mg. Therefore, the graphene percentage in the G/C composite is calculated to be about 32 wt% ((238.22-162)/238.22).

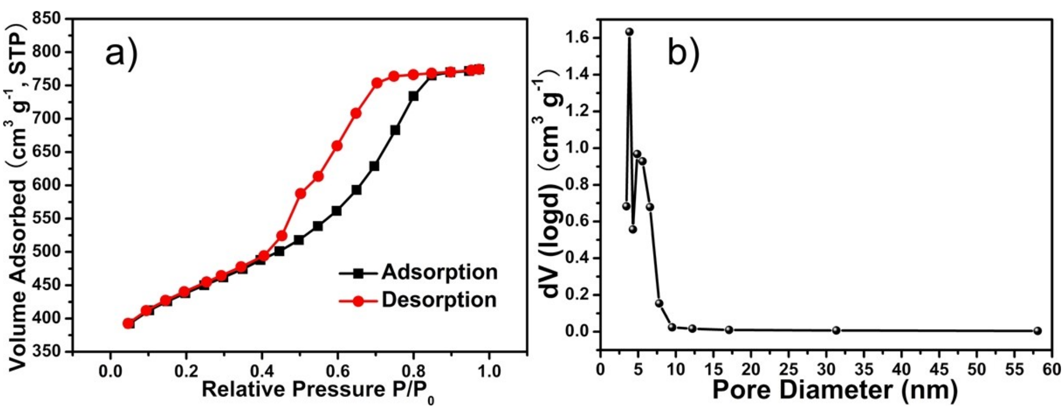

Fig. S6 (a) N_2 adsorption-desorption isotherm and (b) pore size distribution curve of the pure graphene.

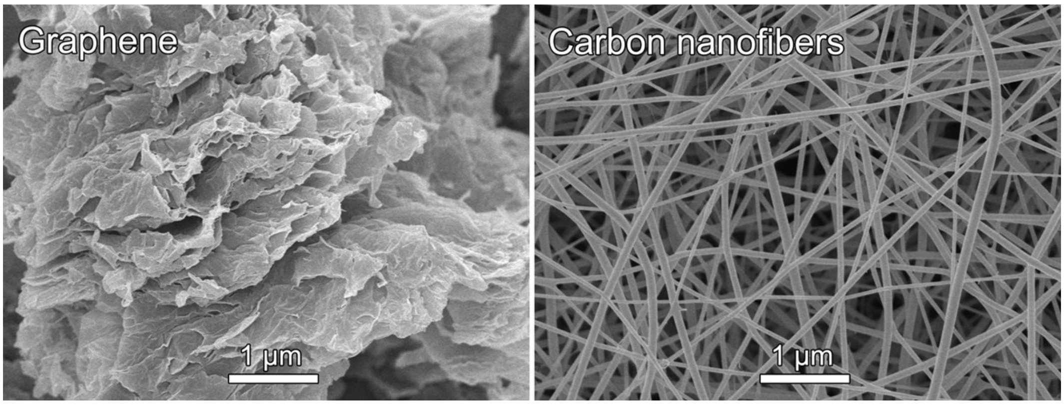

Fig. S7 SEM images of the pure graphene nanosheets and carbon nanofibers.

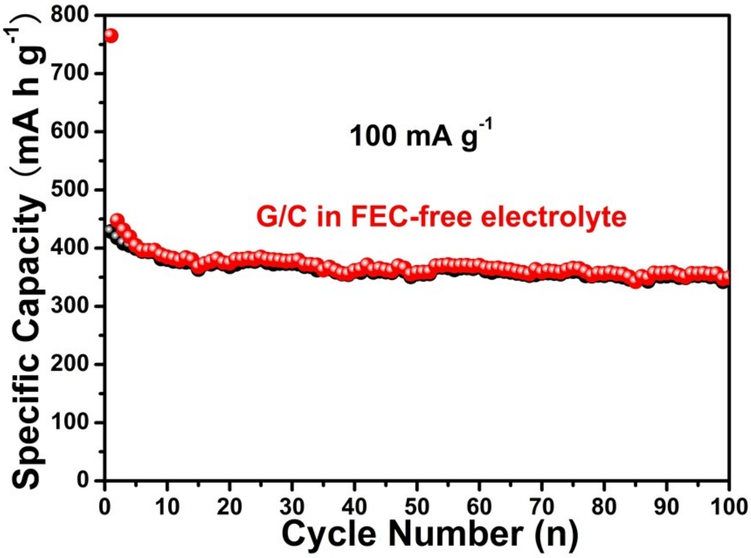

Fig. S8 Cycling performance of the G/C electrode in FEC-free $NaClO_4$/PC electrolyte tested between 0.01-2.5 V vs Na^+/Na at a current density of 100 mA g^{-1}.

The initial discharge and charge capacities are 765 and 428.6 mA h g^{-1}, respectively. While the reversible capacity decreases rapidly to 368.1 mA h g^{-1} in the 20^{th} cycle, and retains only 346.5 mA h g^{-1} after 100 cycles.

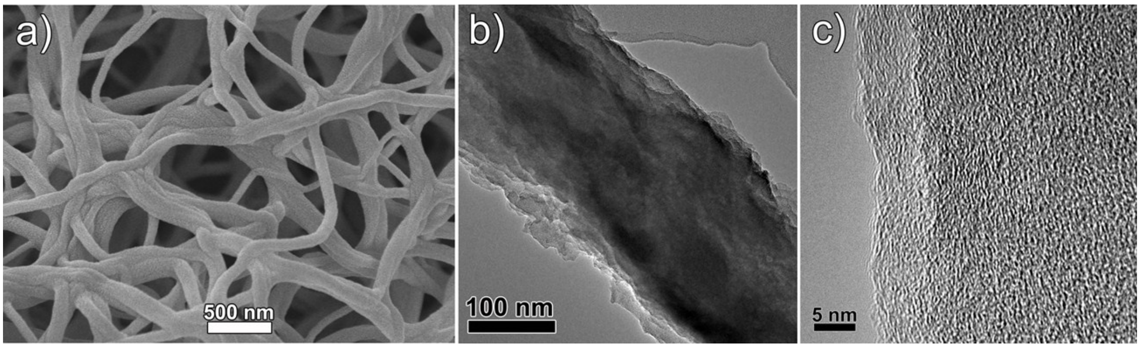

Fig. S9 (a) SEM, (b) TEM, and (c) HRTEM images of the G/C electrode charged at 2.5 V after 300 cycles tested as Fig. 5d.

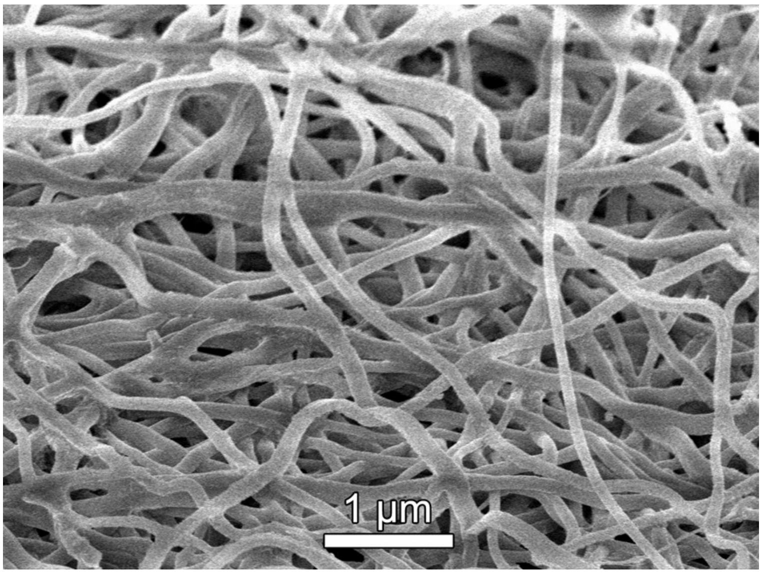

Fig. S10 SEM image of the G/C electrode charged at 2.5 V after 1000 cycles tested at 2000 mA g^{-1}.

Table S1 Comparison of the results in this study with reported performance of the carbon-based materials (including hard carbon, graphene, graphite, heteroatom-doped carbon, and their composites) as SIB anodes.

Sample	Rate capability	Cyclic stability	Reference
Carbonized peat moss	306 mA h g^{-1} at 50 mA g^{-1} 298 mA h g^{-1} at 100 mA g^{-1} 203 mA h g^{-1} at 500 mA g^{-1} 150 mA h g^{-1} at 1000 mA g^{-1} 106 mA h g^{-1} at 2000 mA g^{-1} 66 mA h g^{-1} at 5000 mA g^{-1}	255 mA h g^{-1} at 100 mA g^{-1} (200 cycles)	1
Reduced graphene oxide	217.2 mA h g^{-1} at 40 mA g^{-1} 176.4 mA h g^{-1} at 80 mA g^{-1} 150.9 mA h g^{-1} at 200 mA g^{-1} 118.7 mA h g^{-1} at 400 mA g^{-1} 95.6 mA h g^{-1} at 1000 mA g^{-1}	174.3 mA h g^{-1} at 40 mA g^{-1} 93.3 mA h g^{-1} at 200 mA g^{-1} (250 cycles) 141 mA h g^{-1} at 40 mA g^{-1} (1000 cycles)	2
Expanded graphite	284 mA h g^{-1} at 20 mA g^{-1} 184 mA h g^{-1} at 100 mA g^{-1} 91 mA h g^{-1} at 200 mA g^{-1}	73.92% capacity retention at 100 mA g^{-1} (2000 cycles)	3
Hollow carbon nanospheres	223 mA h g^{-1} at 50 mA g^{-1} 168 mA h g^{-1} at 200 mA g^{-1} 142 mA h g^{-1} at 500 mA g^{-1} 120 mA h g^{-1} at 1000 mA g^{-1} 100 mA h g^{-1} at 2000 mA g^{-1} 75 mA h g^{-1} at 5000 mA g^{-1} ~50 mA h g^{-1} at 10000 mA g^{-1}	~160 mA h g^{-1} at 100 mA g^{-1} (100 cycles)	4
Microporous carbon nanospheres	223 mA h g^{-1} at 20 mA g^{-1} 190 mA h g^{-1} at 200 mA g^{-1} 130 mA h g^{-1} at 100 mA g^{-1} 98 mA h g^{-1} at 200 mA g^{-1} 85 mA h g^{-1} at 400 mA g^{-1} 67 mA h g^{-1} at 1000 mA g^{-1}	115 mA h g^{-1} at 200 mA g^{-1} (1000 cycles)	5
Sandwich-like hierarchically carbon /graphene composite	670 mA h g^{-1} at 50 mA g^{-1}	400 mA h g^{-1} at 50 mA g^{-1} (100 cycles) 250 mA h g^{-1} at 1000 mA g^{-1} (1000 cycles)	6
3D nitrogen-doped graphene foams	1057.1 mA h g^{-1} at 100 mA g^{-1} 943.5 mA h g^{-1} at 200 mA g^{-1} 815.2 mA h g^{-1} at 500 mA g^{-1} 467.1 mA h g^{-1} at 1000 mA g^{-1} 244.7 mA h g^{-1} at 2000 mA g^{-1} 137.7 mA h g^{-1} at 5000 mA g^{-1}	594 mA h g^{-1} at 500 mA g^{-1} (150 cycles)	7
3D porous carbon frameworks	290 mA h g^{-1} at 200 mA g^{-1} 253 mA h g^{-1} at 500 mA g^{-1} 200 mA h g^{-1} at 1000 mA g^{-1} 166 mA h g^{-1} at 2000 mA g^{-1} 130 mA h g^{-1} at 5000 mA g^{-1} 104 mA h g^{-1} at 10000 mA g^{-1} 90 mA h g^{-1} at 20000 mA g^{-1}	256.5 mA h g^{-1} at 500 mA g^{-1} (500 cycles) 150.1 mA h g^{-1} at 2500 mA g^{-1} (3000 cycles) 99.8 mA h g^{-1} at 5000 mA g^{-1} (10000 cycles)	8

Hard carbon	~250 mA h g^{-1} at 25 mA g^{-1}	~230 mA h g^{-1} at 25 mA g^{-1} (100 cycles)	9
Amorphous carbon	254 mA h g^{-1} at 30 mA g^{-1} 212 mA h g^{-1} at 150 mA g^{-1} 162 mA h g^{-1} at 300 mA g^{-1}	226 mA h g^{-1} at 30 mA g^{-1} (150 cycles)	10
Hollow carbon nanowires	252 mA h g^{-1} at 50 mA g^{-1} 238 mA h g^{-1} at 125 mA g^{-1} 216 mA h g^{-1} at 250 mA g^{-1} 149 mA h g^{-1} at 500 mA g^{-1}	206.3 mA h g^{-1} at 50 mA g^{-1} (400 cycles)	11
Graphene-templated carbon	205 mA h g^{-1} at 200 mA g^{-1} 150 mA h g^{-1} at 500 mA g^{-1} 118 mA h g^{-1} at 1000 mA g^{-1} 97 mA h g^{-1} at 2000 mA g^{-1} 68 mA h g^{-1} at 5000 mA g^{-1} 45 mA h g^{-1} at 10000 mA g^{-1}	190 mA h g^{-1} at 200 mA g^{-1} (2000 cycles)	12
Cellulose derived carbon nanofibers	262.9 mA h g^{-1} at 40 mA g^{-1} 85 mA h g^{-1} at 2000 mA g^{-1}	176 mA h g^{-1} at 200 mA g^{-1} (600 cycles)	13
Electrospun carbon nanofibers	233 mA h g^{-1} at 50 mA g^{-1} 180 mA h g^{-1} at 100 mA g^{-1} 173 mA h g^{-1} at 200 mA g^{-1} 136 mA h g^{-1} at 500 mA g^{-1} 113 mA h g^{-1} at 1000 mA g^{-1} 82 mA h g^{-1} at 2000 mA g^{-1}	169 mA h g^{-1} at 200 mA g^{-1} (200 cycles)	14
Functionalized N-doped carbon nanofibers	172 mA h g^{-1} at 50 mA g^{-1} 150 mA h g^{-1} at 200 mA g^{-1} 139 mA h g^{-1} at 500 mA g^{-1} 132 mA h g^{-1} at 1000 mA g^{-1} 121 mA h g^{-1} at 2000 mA g^{-1} 100 mA h g^{-1} at 5000 mA g^{-1} 87 mA h g^{-1} at 10000 mA g^{-1}	134.2 mA h g^{-1} at 200 mA g^{-1} (200 cycles)	15
Electrospun nitrogen-doped carbon nanofibers	293 mA h g^{-1} at 50 mA g^{-1} 159 mA h g^{-1} at 1000 mA g^{-1}	254 mA h g^{-1} at 50 mA g^{-1} 150 mA h g^{-1} at 1000 mA g^{-1} (200 cycles)	16
Porous carbon nanofibers	280 mA h g^{-1} at 50 mA g^{-1} 200 mA h g^{-1} at 1000 mA g^{-1} 164 mA h g^{-1} at 2000 mA g^{-1} 90 mA h g^{-1} at 5000 mA g^{-1} 60 mA h g^{-1} at 10000 mA g^{-1} 40 mA h g^{-1} at 20000 mA g^{-1}	266 mA h g^{-1} at 50 mA g^{-1} (100 cycles) 140 mA h g^{-1} at 500 mA g^{-1} (1000 cycles)	17

N,O-dual doped carbon network	650 mA h g^{-1} at 100 mA g^{-1} 501 mA h g^{-1} at 200 mA g^{-1} 344 mA h g^{-1} at 500 mA g^{-1} 264 mA h g^{-1} at 800 mA g^{-1} 235 mA h g^{-1} at 1000 mA g^{-1} 197 mA h g^{-1} at 2000 mA g^{-1} 180 mA h g^{-1} at 3000 mA g^{-1} 161 mA h g^{-1} at 5000 mA g^{-1}	545 mA h g^{-1} at 100 mA g^{-1} (100 cycles) 240 mA h g^{-1} at 2000 mA g^{-1} (2000 cycles)	18
Nitrogen-doped carbon nanofiber film	315 mA h g^{-1} at 500 mA g^{-1} ~275 mA h g^{-1} at 1000 mA g^{-1} ~170 mA h g^{-1} at 10000 mA g^{-1} 154 mA h g^{-1} at 15000 mA g^{-1}	377 mA h g^{-1} at 100 mA g^{-1} (100 cycles) 210 mA h g^{-1} at 5000 mA g^{-1} (7000 cycles)	19
Graphene/nitrogen-doped porous carbon nanofiber composite	557.1 mA h g^{-1} at 50 mA g^{-1} 180.1 mA h g^{-1} at 100 mA g^{-1} 115.7 mA h g^{-1} at 800 mA g^{-1} 104 mA h g^{-1} at 1600 mA g^{-1}	175.9 mA h g^{-1} at 100 mA g^{-1} 130 mA h g^{-1} at 200 mA g^{-1} (300 cycles) 97.7 mA h g^{-1} at 1000 mA g^{-1} (500 cycles)	20
Nitrogen-doped carbon/graphene	336 mA h g^{-1} at 30 mA g^{-1} 274 mA h g^{-1} at 100 mA g^{-1} 249 mA h g^{-1} at 200 mA g^{-1} 207 mA h g^{-1} at 500 mA g^{-1} 177 mA h g^{-1} at 1000 mA g^{-1} 139 mA h g^{-1} at 2000 mA g^{-1} 94 mA h g^{-1} at 5000 mA g^{-1}	270 mA h g^{-1} at 50 mA g^{-1} (200 cycles)	21
Graphite	~100 mA h g^{-1} at 37.2 mA g^{-1}	~75 mA h g^{-1} at 37.2 mA g^{-1} (1000 cycles)	22
Porous nitrogen-doped carbon sphere	237 mA h g^{-1} at 100 mA g^{-1} 215 mA h g^{-1} at 200 mA g^{-1} 184 mA h g^{-1} at 500 mA g^{-1} 155 mA h g^{-1} at 1000 mA g^{-1}	206 mA h g^{-1} at 200 mA g^{-1} (600 cycles)	23
Hard carbon nanoparticles	275 mA h g^{-1} at 25 mA g^{-1} 266 mA h g^{-1} at 50 mA g^{-1} 236 mA h g^{-1} at 125 mA g^{-1} 181 mA h g^{-1} at 250 mA g^{-1} 72 mA h g^{-1} at 1250 mA g^{-1} 45 mA h g^{-1} at 2500 mA g^{-1}	207 mA h g^{-1} at 50 mA g^{-1} (500 cycles)	24
S-doped N-rich carbon nanosheets	350 mA h g^{-1} at 50 mA g^{-1} 300 mA h g^{-1} at 100 mA g^{-1} 280 mA h g^{-1} at 200 mA g^{-1} 250 mA h g^{-1} at 500 mA g^{-1} 220 mA h g^{-1} at 1000 mA g^{-1} 190 mA h g^{-1} at 2000 mA g^{-1} 150 mA h g^{-1} at 5000 mA g^{-1} 110 mA h g^{-1} at 10000 mA g^{-1}	211 mA h g^{-1} at 1000 mA g^{-1} (1000 cycles)	25
G/C nanofibers	429.4 mA h g^{-1} at 100 mA g^{-1} 401.7 mA h g^{-1} at 200 mA g^{-1} 371.5 mA h g^{-1} at 500 mA g^{-1} 342 mA h g^{-1} at 1000 mA g^{-1} 324.5 mA h g^{-1} at 2000 mA g^{-1} 291.4 mA h g^{-1} at 5000 mA g^{-1} 261.1 mA h g^{-1} at 10000 mA g^{-1}	408.8 mA h g^{-1} at 100 mA g^{-1} (100 cycles) 382.8 mA h g^{-1} at 500 mA g^{-1} (300 cycles) 300.8 mA h g^{-1} at 2000 mA g^{-1} (1000 cycles)	Present work

Supplementary References

1 J. Ding, H. Wang, Z. Li, A. Kohandehghan, K. Cui, Z. Xu, B. Zahiri, X. Tan, E. M. Lotfabad, B. C. Olsen and D. Mitlin, *ACS Nano,* 2013, **7**, 11004.

2 Y.-X. Wang, S.-L. Chou, H.-K. Liu and S.-X. Dou, *Carbon,* 2013, **57**, 202.

3 Y. Wen, K. He, Y. Zhu, F. Han, Y. Xu, I. Matsuda, Y. Ishii, J. Cumings and C. S. Wang, *Nat. Commun.,* 2014, **5**, 4033.

4 K. Tang, L. Fu, R. J. White, L. Yu, M.-M. Titirici, M. Antonietti and J. Maier, *Adv. Energy Mater.,* 2012, **2**, 873.

5 D. Zhou, M. Peer, Z. Yang, V. G. Pol, F. D. Key, J. Jorne, H. C. Foley and C. S. Johnson, *J. Mater. Chem. A,* 2016, **4**, 6271.

6 Y. Yan, Y.-X. Yin, Y.-G. Guo and L.-J. Wan, *Adv. Energy Mater.,* 2014, **4**, 1301584.

7 J. Xu, M. Wang, N. P. Wickramaratne, M. Jaroniec, S. X. Dou and L. M. Dai, *Adv. Mater.,* 2015, **27**, 2042.

8 H. Hou, C. E. Banks, M. Jing, Y. Zhang and X. B. Ji, *Adv. Mater.,* 2015, **27**, 7861.

9 S. Komaba, W. Murata, T. Ishikawa, N. Yabuuchi, T. Ozeki, T. Nakayama, A. Ogata, K. Gotoh and K. Fujiwara, *Adv. Funct. Mater*., 2011, **21**, 3859.

10 Y. Li, Y.-S. Hu, H. Li, L. Q. Chen and X. J. Huang, *J. Mater. Chem. A,* 2016, **4**, 96.

11 Y. L. Cao, L. Xiao, M. L. Sushko, W. Wang, B. Schwenzer, J. Xiao, Z. Nie, L. V. Saraf, Z. Yang and J. Liu, *Nano Lett.,* 2012, **12**, 3783.

12 X. S. Zhou, X. Zhu, X. Liu, Y. Xu, Y. Liu, Z. H. Dai and J. C. Bao, *J. Phys. Chem. C,* 2014, **118**, 22426.

13 W. Luo, J. Schardt, C. Bommier, B. Wang, J. Razink, J. Simonsen and X. L. Ji, *J. Mater. Chem. A,* 2013, **1**, 10662.

14 T. Chen, Y. Liu, L. Pan, T. Lu, Y. Yao, Z. Sun, D. H. C. Chua and Q. Chen, *J. Mater. Chem. A,* 2014, **2**, 4117.

15 Z. Wang, L. Qie, L. Yuan, W. Zhang, X. L. Hu and Y. H. Huang, *Carbon,* 2013, **55**, 328.

16 J. Zhu, C. Chen, Y. Lu, Y. Ge, H. Jiang, K. Fu and X. W. Zhang, *Carbon,* 2015, **94**, 189.

17 W. Li, L. Zeng, Z. Yang, L. Gu, J. Wang, X. Liu, J. Cheng and Y. Yu, *Nanoscale,* 2014, **6**, 693.

18 M. Wang, Z. Yang, W. Li, L. Gu and Y. Yu, *Small,* 2016, **12**, 2559.

19 S. Wang, L. Xia, L. Yu, L. Zhang, H. H. Wang and X. W. Lou, *Adv. Energy Mater.,* 2016, **6**, 1502217.

20 J. Zhang, Z. Zhang and X. Zhao, *RSC Adv.*, 2015, **5**, 104822.

21 H. Liu, M. Jia, B. Cao, R. J. Chen, X. Lv, R. Tang, F. Wu and B. Xu, *J. Power Sources,* 2016, **319**, 195.

22 B. Jache and P. Adelhelm, *Angew. Chem. Int. Ed.,* 2014, **53**, 10169.

23 D. Li, H. Chen, G. Liu, M. Wei, L.-X. Ding, S. Wang and H. Wang, *Carbon,* 2015, **94**, 888.

24 L. F. Xiao, Y. L. Cao, W. A. Henderson, M. L. Sushko, Y. Shao, J. Xiao, W. Wang, M. H. Engelhard, Z. Nie and J. Liu, *Nano Energy,* 2016, **19**, 279.

25 J. Yang, X. Zhou, D. Wu, X. Zhao and Z. Zhou, *Adv. Mater.,* 2016, DOI: 10.1002/adma.201604108.